Chapter 3

Robust Accelerating Control for Consistent Node Dynamics in a Platoon of CAVs

Feng Gao, Shengbo Eben Li and Keqiang Li

Additional information is available at the end of the chapter

http://dx.doi.org/10.5772/63352

Abstract

Driving as a platoon has potential to significantly benefit traffic capacity and safety. To generate more identical dynamics of nodes for a platoon of automated connected vehicles (CAVs), this chapter presents a robust acceleration controller using a multiple model control structure. The large uncertainties of node dynamics are divided into small ones using multiple uncertain models, and accordingly multiple robust controllers are designed. According to the errors between current node and multiple models, a scheduling logic is proposed, which automatically selects the most appropriate candidate controller into loop. Even under relatively large plant uncertainties, this method can offer consistent and approximately linear dynamics, which simplifies the synthesis of upper level platoon controller. This method is validated by comparative simulations with a sliding model controller and a fixed $\mathbf{H}_\infty$ controller.

Keywords: automated connected vehicles (CAVs), platoon control, acceleration control, robustness, multi-model

1. Introduction

The platoon driving of automated connected vehicles (CAVs) has considerable potential to benefit road traffic, including increasing highway capacity, less fuel/energy consumption and fewer accidents [1]. The R&D of CAVs has been accelerated with increasing usage of wireless communication in road transportation, such as dedicated short range communications (DSRC). Pioneering studies on how to control a platoon of CAVs can date back to 1990s, and as pointed out by Hedrick et al. , the control topics of a platoon can be divided into two tasks [2, 3]: (1) to implement control of platoon formation, stabilization and dissolution; and (2) to carry out

controls for throttle/brake actuators of each vehicle [4]. These naturally lead to a hierarchical control structure, including an upper level controller and a lower level controller [5, 6]. The upper one is to retain safe and string stable operation, whereas the lower one is to track the desired acceleration by determining throttle/brake commands.

The upper level control of a platoon of CAVs has been investigated extensively. An earlier work done by Shladover [2] introduced many known control topics, among which the most famous is the concept of string stability. The string stability ensures that range errors decrease as propagating along downstream [7]. Stankovic et al. [8] proposed a decentralized overlapping control law by using the inclusion principle, which decomposes the original system into multiple ones by an appropriate input/state expansion. Up to now, many other upper level control topics have already been explored, including the influence of spacing policies, information flow topologies, time delay and data loss of wireless communications, etc.

The lower level controller determines the commands for throttle and/or brake actuators. The lower level controller, together with vehicle itself, actually plays the role of node dynamics for upper level control. Many research efforts have been attempted on acceleration control in the past decades, but still few gives emphasis on the request of platoon level automation. Most platoon control relies on one critical assumption that the node dynamics are homogeneous and approximately linear. Then, the node dynamics can be described by simple models, e.g. double-integrator [9, 10] and three-order model [3, 7, 8, 11]. This requires that the behaviour of acceleration control is rather accurate and consistent, which is difficult to be achieved. One is because the salient non-linearities in powertrain dynamics, both traditional [12, 13] and hybridized [14], and any linearization, will lead to errors; the other is that such uncertainties as parametric variations and external disturbances significantly affect the consistence of control behaviour.

One of the major issues of acceleration control is how to deal with non-linearities and uncertainties. The majority to handle non-linearities are to linearize powertrain dynamics, including exact linearization [15, 16], Taylor linearization [17] and inverse model compensation [12, 18]. Fritz and Schiehlen [15, 16] use the exact linearization technique to normalize node dynamics for synthesis of cruising control. After linearization, a pole placement controller was employed to control the exactly linearized states. The Taylor expansion approach has been used by Hunt et al. [17] to approximate the powertrain dynamics at equilibrium points. The gain-scheduling technique was then used to conquer the discrepancy caused by linearization. The inverse model compensation is widely used in engineering practice, for example [12] and [19]. This method is implemented by neglecting the powertrain dynamics. For the uncertainties, the majority rely on robust control techniques, including sliding model control (SMC) [19], $\mathbf{H}_\infty$ control [20, 21], adaptive control [22–24], fuzzy control [25, 26], etc. Considering parametric variations, an adaptive SMC was designed by Swaroop et al. [19] by adding an on-line estimator for vehicle parameters, such as mass, aerodynamic drag coefficient and rolling resistance. Higashimata and Adachi [20] and Yamamura and Seto [21] designed a Model Matching Controller (MMC) based controller for headway control. This design used an $\mathbf{H}_\infty$ controller as feedback and a forward compensator for a faster response. Xu and Ioannou [23] approximated vehicle dynamics to be a first-order transfer function at equilibrium points, and

http://dx.doi.org/10.5772/63352

then the Lyapunov approach was used to design an adaptive thriller controller for tracking control of vehicle speed. Keneth et al (2008) designed an adaptive proportional-integral (PI) controller for robust tracking control in resistance to parametric variations. The adaptive law is designed by using the gradient algorithm [24]. The aforementioned robust controllers are useful to resist small errors and disturbances in vehicle longitudinal dynamics, but might not be always effective for large uncertainties. Moreover, the use of adaptive mechanism is only able to resist slowly varying uncertainties, but difficult to respond fast varying disturbances, e.g. instantaneous wind.

2. Node dynamic model for control

This chapter proposes a robust acceleration control method for consistent node dynamics in a platoon of CAVs. This design is able to offer more consistent and approximately linear node dynamics for upper level control of platoons even under large uncertainties, including vehicle parametric variation, varying road slop and strong environmental wind. The controlled node in the platoon is a passenger car with a 1.6 L gasoline engine, a 4-speed automatic transmission, two driving and two driven wheels, as well as a hydraulic braking system. **Figure 1** presents the powertrain dynamics. Its inputs are the throttle angle $\boldsymbol{\alpha}_{\mathbf{thr}}$ and the braking pressure $\boldsymbol{P}_{\mathbf{brh}}$. Its outputs are the longitudinal acceleration $\boldsymbol{a}$, vehicle velocity $\boldsymbol{v}$, as well as other measurable variables in the powertrain. When driving, the engine torque is amplified by the automatic transmission, final gear, and then acts on two frontal driving wheels. When braking, the braking torque acts on four wheels to dissipate the kinetic energy of vehicle body.

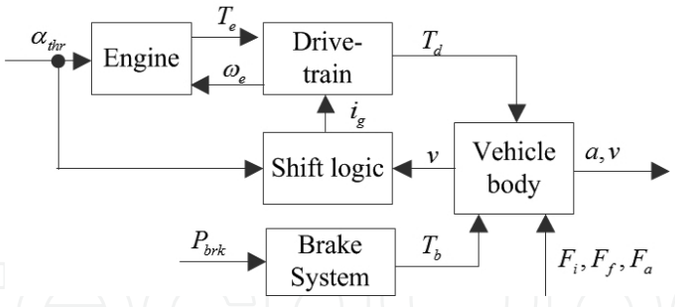

Figure 1. Vehicle longitudinal dynamics.

2.1. Vehicle longitudinal dynamics

For the sake of controller design, it is further assumed that (1) the dynamics of intake manifold and chamber combustion are neglected, and overall engine dynamics are lumped into a first-order inertial transfer function; (2) the vehicle runs on dry alphabet roads with high road-tyre friction, and so the slip of tire is neglected; (3) the vehicle body is considered to be rigid and symmetric, without vertical motion, yaw motion and pitching motion; (4) the hydraulic braking system is simplified to a first-order inertial transfer function without time delay. Then, the mathematical model of vehicle longitudinal dynamics is

$$
\begin{aligned}
&T_{es} = \mathbf{MAP}\left(\omega_e, \alpha_{thr}\right), T_e = \frac{1}{\tau_e s + 1} T_{es}, J_e \dot{\omega}_e = T_e - T_p, \\
&T_p = C_{TC} \omega_e^2, T_t = K_{TC} T_p, T_d = \eta_T i_g i_0 T_t, \omega_t = i_g i_0 \frac{v}{r_w}, \\
&M\dot{v} = \frac{T_d}{r_w} - \frac{T_b}{r_w} - F_i - F_a - F_f, T_b = \frac{K_b}{\tau_b s + 1} P_{brk}, F_i = Mg \cdot \sin(\varphi), \\
&F_a = \text{sign}\left(v + v_{wind}\right) C_A \left(v + v_{wind}\right)^2, F_f = Mg \cdot f,
\end{aligned}
\tag{1}
$$

where ω_e is the engine speed, T_{es} is the static engine torque, τ_e is the time constant of engine dynamics, $\mathbf{T_e}$ is the actual engine torque, $\mathbf{MAP}_{(.,.)}$ is a non-linear tabular function representing engine torque characteristics, T_p is the pump torque of torque converter (TC), J_e is the inertia of fly wheel, T_t is the turbine torque of TC, C_{Tc} is the TC capacity coefficient, K_{TC} is the torque ratio of TC, i_g is the gear ratio of transmission, i_o is the ratio of final gear, η_T is the mechanical efficiency of driveline, r_w is the rolling radius of wheels, M is the vehicle mass, T_d is the driving force on wheels, T_b is the braking force on wheels, v is the vehicle speed, F_i is the longitudinal component of vehicle gravity, F_a is the aerodynamic drag, F_f is the rolling resistance, K_b is the total braking gain of four wheels, τ_b is the time constant of braking system, C_A is the coefficient of aerodynamic drag, g is the gravity coefficient, f is the coefficient of rolling resistance, ϕ is the road slope and v_{wind} is the speed of environmental wind. The nominal values of vehicle parameters are shown in **Table 1**.

Symbol	Units	Nominal value
M	Kg	1300
J_e	kg·m^2	0.21
η_T	–	0.89
τ_e	Sec	0.3
i_o	–	4.43
i_g	–	[2.71, 1.44, 1, 0.74]
r_w	M	0.28
K_b	N·m/MPa	1185
τ_b	Sec	0.15
C_A	kg/m	0.2835
f	–	0.02
g	m/s^2	9.81

Table 1. Nominal parameters of vehicle model.

http://dx.doi.org/10.5772/63352

2.2. Inverse vehicle model

One major challenge of acceleration control is the salient non-linearities, including engine static non-linearity, torque converter coupling, discontinuous gear ratio, quadratic aerodynamic drag and the throttle/brake switching. These non-linearities can be compensated by an inverse vehicle model. The inverse models of engine and brake are described by Eqs. (2) and (3), respectively [22, 31]. The design of the inverse model assumes that (i) engine dynamics, torque converter coupling, etc. is neglected; (ii) vehicle runs on dry and flat road with no mass transfer; (iii) the inverse model uses nominal parameters in **Table 1**.

$$T_{\text{edes}} = \frac{r_w}{i_g i_0 \eta_T}\left(Ma_{\text{des}} + C_A v^2 + Mgf\right), \alpha_{\text{thrdes}} = \text{MAP}^{-1}\left(\omega_e, T_{\text{edes}}\right), \tag{2}$$

$$F_{\text{bdes}} = Ma_{\text{des}} + C_A v^2 + Mgf, P_{\text{brkdes}} = \frac{1}{K_b} F_{\text{bdes}}, \tag{3}$$

where a_{des} is the input for the inverse model, which is the command of acceleration control, T_{edes}, α_{thrdes}, F_{bdes} and P_{brkdes} are corresponding intermittent variables or actuator commands. Note that throttle and braking controls cannot be applied simultaneously. A switching logic with a hysteresis layer is required to determine which one is used. The switching line for separation is not simply to be zero, i.e. $a_{\text{des}} = 0$, because the engine braking and the aerodynamic drag are firstly used, and followed by hydraulic braking if necessary. Therefore, the switching line is actually equal to the deceleration when coasting, shown in **Figure 2**. The use of a hysteresis layer is to avoid frequent switching between throttle and brake controls.

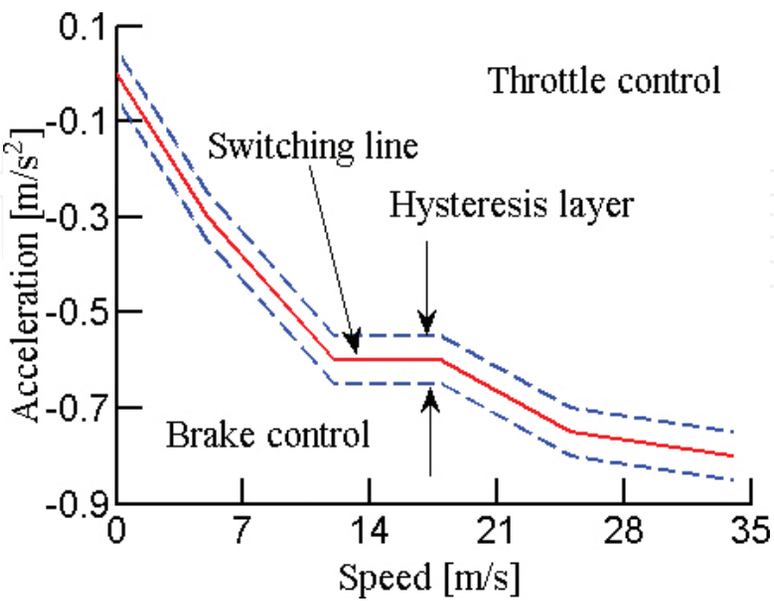

Figure 2. Switching between throttle and brake controls.

3. MMS-based acceleration control

The Multi Model Switching (MMS) control is an efficient way to control plants with large model uncertainties and linearization errors, especially sudden changes in plant dynamics [27–30]. The overall range of plant dynamics is covered by a set of models instead of a single one, and then a scheduling logic switches the most appropriate controller into the control loop. The speed of adaptation and transient performance can be significantly improved by the instantaneous switching among candidate controllers [29, 30]. Another benefit of MMS control is its potential to enclose the input-output behaviours to a required small range. **Figure 3** shows the MMS control structure for vehicle acceleration tracking, where $\boldsymbol{a}_{\mathbf{des}}$ and $\boldsymbol{a}$ are the desired and actual longitudinal acceleration respectively, $\boldsymbol{\alpha}_{thrdes}$ and $\boldsymbol{P}_{brkdes}$ are throttle angle and braking pressure respectively, which are the control inputs of a vehicle. It consists of the vehicle itself (**V**), the inverse model (**I**), a supervisor (**S**) and a controller set (**C**). The inverse model **I** is used to compensate for the non-linearities of powertrain; **I** and **V** together constructs the plant for MMS control. The combination of **I + V** tends to have large uncertainties, but is divided into small ones under the MMS structure. Such a configuration is able to maintain a more accurate and consistent input–output behaviour even under a large model mismatch.

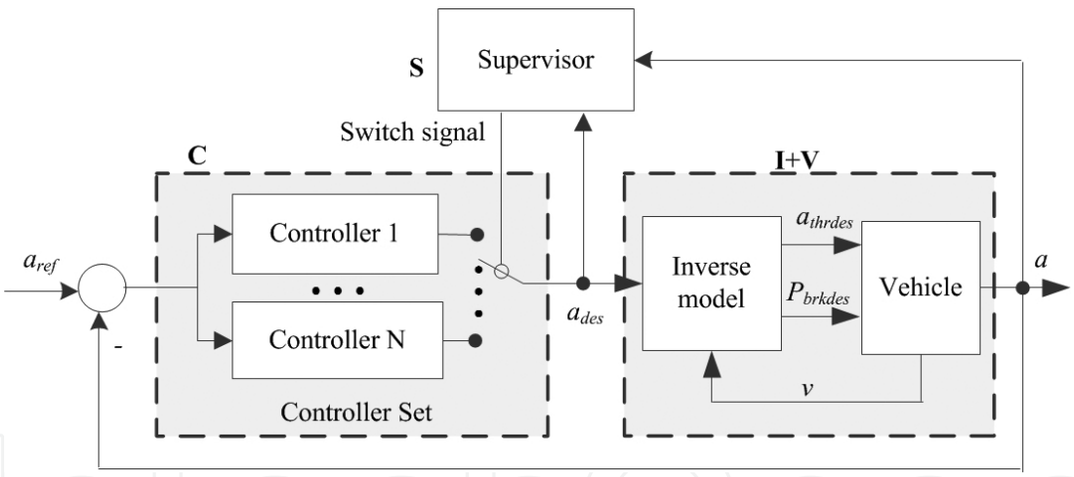

Figure 3. MMS control of vehicle acceleration.

3.1. Model set to separate large uncertainty

For the MMS control, **I** and **V** are combined together to form a new plant, whose input is desired acceleration and output is actual acceleration. Its major uncertainties arise from the change of operating speed, i.e. $v \in \mathbb{R}^1$, the parameter variation, i.e. $\theta = [M,\ \eta_T,\ \tau_e,\ K_b] \in \mathbb{R}^4$. and the external disturbance, i.e. $d = [\varphi,\ v_{\text{wind}}] \in \mathbb{R}^2$. Their uncertain range is $v \in [v_{\min},\ v_{\max}]$, $\theta \in [\theta_{\min},\ \theta_{\max}]$ and $d \in [d_{\min},\ d_{\max}]$. The main idea is to use multiple linear models, i.e. $P_i(s)$, $i = 1, \cdots, N$, to separate such large uncertainties into small ones, and accordingly design multiple feasible $\mathbf{H}_\infty$ controllers, i.e. $C_i(s)$, $i = 1, \cdots, N$, for each model with smaller uncertainty.

http://dx.doi.org/10.5772/63352

The range of vehicle speed, $v \in \mathbb{R}$, is equally divided into five points, i.e. $\left(v_{\min}, \frac{3v_{\min}+v_{\max}}{4}, \frac{2v_{\min}+2v_{\max}}{4}, \frac{v_{\min}+3v_{\max}}{4}, v_{\max}\right)$, and the range of $\theta \in \mathbb{R}^4$ and $d \in \mathbb{R}^2$ are each separated into three points, i.e. $\left(\theta_{\min}, \frac{\theta_{\min}+\theta_{\max}}{2}, \theta_{\max}\right)$, and $\left(d_{\min}, \frac{d_{\min}+d_{\max}}{2}, d_{\max}\right)$, respectively. Their combination is set as a candidate for model identification. Totally, there are $5\times3^{(4+2)}=3465$ candidate models. The 3465 models can be straightforwardly regarded as a multiple model set. Its shortcoming is that some of these models are quite closed to each other, which naturally leads to many redundant controllers (a waste of computing and storage resources). To reduce the model number, some close models are grouped and covered by an uncertain model. Hence, these 3465 models are clustered into four groups, which are covered with four uncertain models $P_i(s)$, $i=1, \cdots, N$, shown in **Figure 4**.

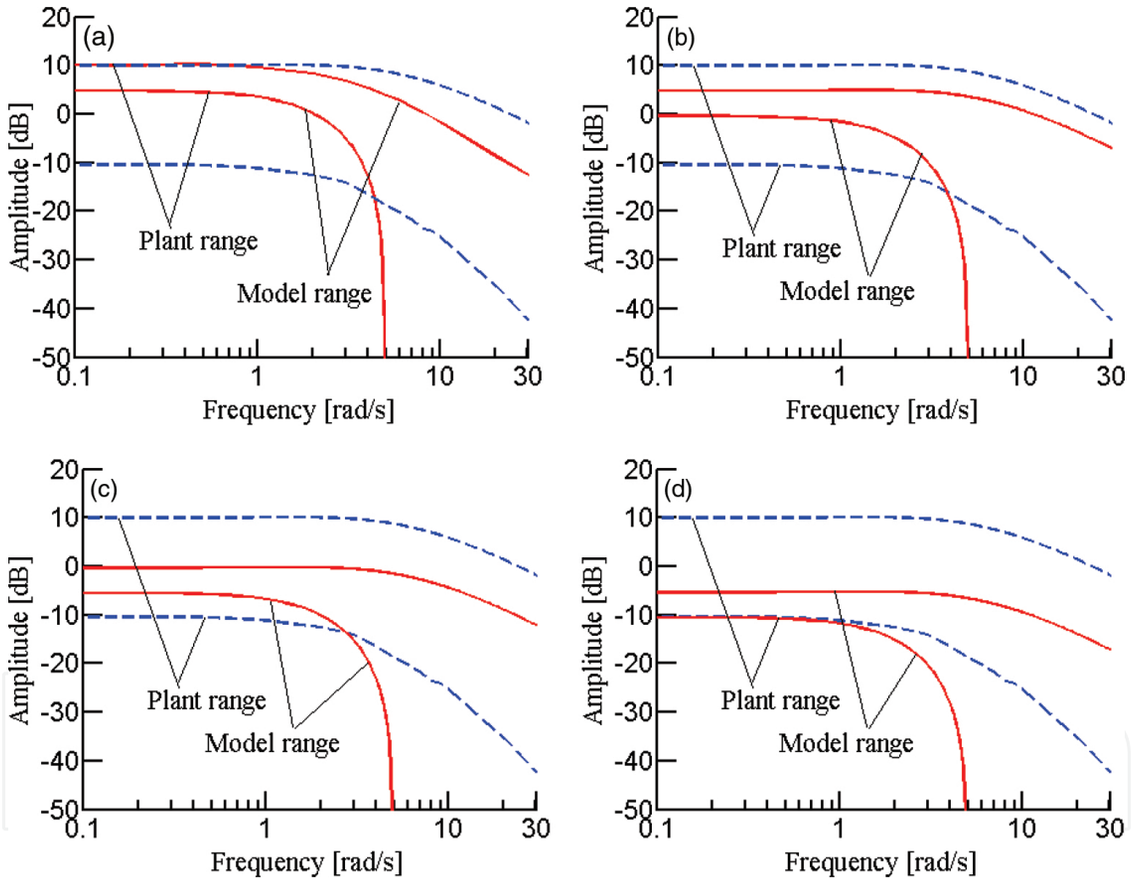

Figure 4. Frequency responses of four linear models. (a) Model $P_1(s)$, (b) Model $P_2(s)$, (c) Model $P_3(s)$ and (d) Model $P_4(s)$.

The model set $\mathbf{P}=\{P_i(s), i=1, \cdots, N\}$ is defined to have identical structure with a multiplicative uncertainty:

$$P_i(s) = G_i(s)\left[1+\Delta_i W(s)\right], G_i(s) = k_{Gi}\left(s+p_G\right)^{-1}, i=1\cdots N, \tag{4}$$

where $G_i(s)$ is the nominal models listed in **Table 2**, $W(s)$ is the weight function for uncertainty, Δ_i is the model uncertainty, satisfying:

$$\left\|\Delta_i\right\|_\infty^\delta < 1, i = 1 \cdots N, \tag{5}$$

where $\|\cdot\|_\infty^\delta$ is the induced norm of $\mathbf{L}_2^\delta$ norm of signals expressed as

$$\left\|\mathbf{x}(t)\right\|_2^\delta = \sqrt{\int_0^t e^{-\delta(t-\tau)} \left|\mathbf{x}(t)\right|^2 d\tau}, \tag{6}$$

where $\delta > 0$ is a forgetting factor, and $\mathbf{x}(t)$ is a vector of signals.

No.	**1**	**2**	**3**	**4**
$G_i(s)$	$\frac{8.15}{s + 3.333}$	$\frac{4.5}{s + 3.333}$	$\frac{0.75}{s + 3.333}$	$\frac{0.22}{s + 3.333}$

Table 2. Nominal models of node dynamics.

3.2. Synthesis of the MMS controller

The main idea of this chapter is to use multiple uncertain models to cover overall plant dynamics, and so the large uncertainty is divided into smaller ones. Because the range of dynamics covered by each model is reduced using multiple models, this MMS control can greatly improve both robust stability and tracking performance of vehicle acceleration control. This MMS controller includes a scheduling logic **S**, multiple estimators **E** and multiple controllers **C**. The module **E** is a set of estimators, which is designed from model set **P** and to estimate signals a and z. Note that z is the disturbance signal arising from model uncertainty and it cannot be measured directly. The module **S** represents the scheduling logic. Its task is to calculate and compare the switching index of each model $J_i (i = 1, \cdots, N)$, which actually gives a measure of each model uncertainty compared with current vehicle dynamics. **S** chooses the most proper model (with smallest measure) and denoted as σ. The module **C** contains multiple robust controllers, also designed from **P**. The controller whose index equals σ will be switched into loop to control acceleration. The signal a_{ref} is the desired acceleration.

The scheduling logic is critical to the MMS controller, because it evaluates errors between current vehicle dynamics and each model in **P**, and determines which controller should be chosen. The controller index σ is determined by:

$$\sigma = \arg\min_{i=1,\cdots,4} J_i(t). \tag{7}$$

Intuitively, $J_i(t)$ is designed to measure the model uncertainty σ_t, and so the estimator set $\mathbf{E}=\{E_i,\ i=1,\ \cdots,\ N\}$ is designed to indirectly measure σ_i as follows:

$$\hat{z}_i = -\frac{k_{Gi}}{\Lambda(s)} W(s) a_{\text{des}},\ \hat{a}_i = \frac{k_{Gi}}{\Lambda(s)} a_{\text{des}} + \frac{\Lambda(s) - (s + p_G)}{\Lambda(s)} a, i = 1, \cdots, 4, \tag{8}$$

where $\Lambda(s)$ is the common characteristic polynomial of $\mathbf{E}$, $\hat{a}_i$ and $\hat{z}_i$ are the estimates of a and z using model P_i. It is easy to know that the stability of estimators can be ensured by properly selecting $\Lambda(S)$. Subtracting Eq. (8) with Eq. (4) yields the estimation error of a:

$$e_i = \hat{a}_i - a = -\frac{k_{Gi}}{\Lambda(s)} W(s) \Delta_i a_{\text{des}} = \Delta_i \hat{z}_i. \tag{9}$$

Then, the switching index $J_i(t)$ is designed to be

$$J_i(t) = \left(\left\| e_i(t) \right\|_2^{\delta} \right)^2 - \left(\left\| \hat{z}_i(t) \right\|_2^{\delta} \right)^2, i = 1, \cdots, 4. \tag{10}$$

Since the system gain from $\hat{z}_\sigma(t)$ to $e_\sigma(t)$ can be bounded by $\mathbf{S}$, $\hat{z}_\sigma(t)$ and $e_\sigma(t)$ can be treated as the input and output of an equivalent uncertainty. Considering Eq. (8), $\mathbf{E}$ is rewritten into

$$\begin{aligned} \dot{\mathbf{x}}_{\text{E}} &= \mathbf{A}_{\text{E}} \mathbf{x}_E + \mathbf{B}_{\text{E1}} a_{\text{des}} + \mathbf{B}_{\text{E2}} a \\ \hat{a}_i &= \mathbf{C}_{\text{E1}i} \mathbf{x}_{\text{E}}, \hat{z}_i = \mathbf{C}_{\text{E2}i} \mathbf{x}_{\text{E}}, \end{aligned} \tag{11}$$

where A_E, B_{E1}, B_{E2}, C_{E11}, C_{E12}, C_{E13}, C_{E14}, C_{E21}, C_{E22}, C_{E23}, C_{E24} are matrices with proper dimensions. By selecting weighting function as $W_{\text{p}}(s) = (0.1s + 1.15)/s$, the required tracking performance becomes:

$$\left\|q(t)\right\|_2^{\delta} < \gamma \left\|a_{\text{ref}}(t)\right\|_2^{\delta}, \tag{12}$$

where a_{ref} is the reference acceleration, $q = W_{\text{p}}(s)e_{\text{a}}$ and $e_{\text{a}} = a_{\text{ref}} - a$, , which is expected to converge to zero. Substituting $a = \hat{a}_{\sigma} - e_{\sigma}$ and Eq. (12) to Eq. (11), we have,

$$\dot{\mathbf{x}} = \mathbf{A}_{\sigma}\mathbf{x} + \mathbf{B}_1 e_{\sigma} + \mathbf{B}_2 a_{\text{des}} + \mathbf{B}_3 a_{\text{ref}} \tag{13}$$

$$\hat{z}_{\sigma} = \mathbf{C}_{1\sigma}\mathbf{x}, q = \mathbf{C}_{2\sigma}\mathbf{x} + D_{\text{p}} e_{\sigma} + D_{\text{p}} a_{\text{ref}}, e_{\text{a}} = \mathbf{C}_{3\sigma}\mathbf{x} + e_{\sigma} + a_{\text{ref}},$$

where $\mathbf{A}_{\sigma} = \begin{bmatrix} \mathbf{A}_{\text{E}} + \mathbf{B}_{\text{E2}}\mathbf{C}_{\text{E1}\sigma} & 0 \\ -\mathbf{C}_{\text{E1}\sigma} & 0 \end{bmatrix}$, $\mathbf{B}_1 = \begin{bmatrix} -\mathbf{B}_{\text{E2}} \\ -1 \end{bmatrix}$, , $\mathbf{B}_2 = \begin{bmatrix} \mathbf{B}_{\text{E1}} \\ 0 \end{bmatrix}$, $\mathbf{B}_3 = \begin{bmatrix} 0 \\ 1 \end{bmatrix}$, $\mathbf{C}_{1\sigma} = [\mathbf{C}_{\text{E2}\sigma} \quad 0]$, $\mathbf{C}_{2\sigma} = [-0.1\mathbf{C}_{\text{E1}\sigma} \quad 1.15]$, $\mathbf{C}_{3\sigma} = [-\mathbf{C}_{\text{E1}\sigma} \quad 0]$, $\mathbf{D}_{31} = 1$, $\mathbf{x} = \begin{bmatrix} \mathbf{x}_{\text{E}} \\ x_p \end{bmatrix}$ are system matrices with proper dimensions. The required robust controller set can be designed by numerically solving the following LMIs:

$$\begin{bmatrix} \mathbf{A}_{\delta i}\mathbf{P}_1 + \mathbf{P}_1\mathbf{A}_{\delta i}^{\text{T}} + \mathbf{B}_2\tilde{\mathbf{C}}_i + \tilde{\mathbf{C}}_i^{\text{T}}\mathbf{B}_2^{\text{T}} & * \\ \left(\tilde{\mathbf{A}}_i + \mathbf{A}_{\delta i} + \mathbf{B}_2\tilde{\mathbf{D}}_i\mathbf{C}_{3i}\right)^{\text{T}} & \mathbf{P}_2\mathbf{A}_{\delta i} + \mathbf{A}_{\delta i}^{\text{T}}\mathbf{P}_2 + \tilde{\mathbf{B}}_i\mathbf{C}_{3i} + \mathbf{C}_{3i}^{\text{T}}\tilde{\mathbf{B}}_i^{\text{T}} \\ \left(\mathbf{B}_2\tilde{\mathbf{D}}_i + \mathbf{B}_1\right)^{\text{T}} & \left(\mathbf{P}_2\mathbf{B}_1 + \tilde{\mathbf{B}}_i\right)^{\text{T}} \\ \left(\mathbf{B}_2\tilde{\mathbf{D}}_i + \mathbf{B}_3\right)^{\text{T}} & \left(\mathbf{P}_2\mathbf{B}_3 + \tilde{\mathbf{B}}_i\right)^{\text{T}} \\ \mathbf{C}_{1i}\mathbf{P}_1 & \mathbf{C}_{1i} \\ \mathbf{C}_{2i}\mathbf{P}_1 & \mathbf{C}_{2i} \end{bmatrix} \tag{14}$$

$$\begin{bmatrix} * & * & ** \\ * & * & ** \\ -\beta^2\mathbf{I} & 0 & ** \\ 0 & -\gamma^2\mathbf{I} & ** \\ 0 & 0 & \mathbf{I}\,0 \\ D_p & D_p & 0\,\mathbf{I} \end{bmatrix} < 0, i = 1, \cdots, 4, \begin{bmatrix} \mathbf{P}_1 & \mathbf{I} \\ \mathbf{I} & \mathbf{P}_2 \end{bmatrix} > 0,$$

where $\beta < 1$ is a positive constant, $\mathbf{A}_{\delta i} = \mathbf{A}_i + 0.5\delta\mathbf{I}$, symbol "*" represents the symmetrical part. Then the controller set $\mathbf{C}$ is

$$\mathbf{C} = \left\{ K_i : \begin{array}{l} \dot{\mathbf{X}}_C = \mathbf{A}_{Ci}\mathbf{X}_C + \mathbf{B}_{Ci}e_{\mathrm{a}} \\ a_{des} = \mathbf{C}_{Ci}\mathbf{X}_C + \mathbf{D}_{Ci}e_{\mathrm{a}} \end{array}, i = 1, \cdots, N \right\}. \tag{15}$$

The matrices in Eq. (15) are calculated as:

$$\begin{aligned} \mathbf{D}_{Ci} = \tilde{\mathbf{D}}_i, \mathbf{C}_{Ci} &= \left(\tilde{\mathbf{C}}_i - \mathbf{D}_{Ci}\mathbf{C}_{3i}\mathbf{P}_1 \right) \left(\mathbf{M}^{\mathrm{T}} \right)^{-1}, \mathbf{B}_{Ci} \\ &= \mathbf{N}^{-1} \left(\tilde{\mathbf{B}}_i - \mathbf{P}_2\mathbf{B}_2\mathbf{D}_{Ci} \right), \end{aligned} \tag{16}$$

$$\begin{aligned} \mathbf{A}_{Ci} = \mathbf{N}^{-1} &\left[\tilde{\mathbf{A}}_i - \mathbf{P}_2 \left(\mathbf{A}_{\delta i} + \mathbf{B}_2\mathbf{D}_{Ci}\mathbf{C}_{3i} \right) \mathbf{P}_1 \right] \left(\mathbf{M}^{\mathrm{T}} \right)^{-1} \\ &-0.5\delta\mathbf{I} - \mathbf{B}_{Ci}\mathbf{C}_{3i}\mathbf{P}_1 \left(\mathbf{M}^{\mathrm{T}} \right)^{-1} - \mathbf{N}^{-1}\mathbf{P}_2\mathbf{B}_2\mathbf{C}_{Ci}, \; i = 1, \cdots, 4, \end{aligned}$$

where $\mathbf{M}$ and $\mathbf{N}$ are the singular value decomposition of $\mathbf{I} - \mathbf{P}_1\mathbf{P}_2$. The controller set $\mathbf{C}$, solved by LMIs Eq. (14), is listed as follows:

$$\mathbf{C} = \left\{ K_1(s), K_2(s), K_3(s), K_4(s) \right\}$$

$$\begin{aligned} K_1(\mathrm{s}) &= \frac{137.1(\mathrm{s} + 4.9)(\mathrm{s} + 3.133)}{s(\mathrm{s} + 41.85)(\mathrm{s} + 45.70)}, \; K_2(\mathrm{s}) \\ &= \frac{233.4(\mathrm{s} + 4.9)(\mathrm{s} + 3.133)}{\mathrm{s}(\mathrm{s} + 80.06)(\mathrm{s} + 21.42)}, \end{aligned} \tag{17}$$

$$\begin{aligned} K_3(\mathrm{s}) &= \frac{573.0(\mathrm{s} + 4.9)(\mathrm{s} + 3.133)}{\mathrm{s}(\mathrm{s} + 29.63)(\mathrm{s} + 99.30)}, \; K_4(\mathrm{s}) \\ &= \frac{283.4(\mathrm{s} + 4.9)(\mathrm{s} + 3.133)}{\mathrm{s}(\mathrm{s} + 54.15)(\mathrm{s} + 19.89)} \end{aligned}$$

4. Simulation results and analyses

To validate the improvements MMS controller for tracking of acceleration, two other controllers are designed, i.e. a sliding mode controller (SMC), and a single $\mathbf{H}_\infty$ controller.

4.1. Design of SMC and $\mathbf{H}_\infty$ controllers

It is known that SMC has high robustness to uncertainties. It is designed based on the nominal model $G_M(s)=0.33/(s+0.33)$. The sliding surface is selected to be

$$e(t)=a-a_{\text{ref}},\ s=\int_0^t e(t)dt+\lambda e(t), \tag{18}$$

where $\lambda>0$. The reaching law is designed to be $\dot{s}=-ks+\eta\text{sgn}(s)$, where $k<0$ and $\eta>0$. Then the sliding mode controller is

$$a_{\text{des}}=\frac{\tau_i}{\lambda k_i}\left[\lambda\dot{a}_{\text{ref}}+\lambda\frac{1}{\tau_i}a-e-ks+\eta\text{sgn}(s)\right] \tag{19}$$

$\mathbf{H}_\infty$ control is another widely used and effective approach to deal with model uncertainties. Here, a model matching control structure is applied to balance between robustness and fastness. The uncertain model of vehicle dynamics used for design of $\mathbf{H}_\infty$ controller is

$$P(s)=\frac{0.3s+1}{0.2s^2+0.6s+1}\left(1+\frac{5.2s+5}{2s+10}\Delta\right),\|\Delta\|_\infty<1 \tag{20}$$

The referenced acceleration response dynamics is $G_M(s)=1/(s+1)$. Then, the feed-forward controller designed by the model matching technique is

$$C_F(s)=\frac{0.2s^2+0.6s+1}{0.3s^2+1.3s+1} \tag{21}$$

The feedback controller designed by the $\mathbf{H}_\infty$ control method is

$$C_B(s)=\frac{6.5493(s+5)(s+6)(s^2+3s+5)}{s(s+10.39)(s+4.74)(s^2+7.049s+14.03)} \tag{22}$$

This $\mathbf{H}_\infty$ controller is numerically solved by the Matlab command *mixsyn*(), with the weighting function $W_p(s)=(0.1s+1.15)s^{-1}$.

4.2. Simulations and analyses

A naturalistic acceleration from real traffic flow is used as the reference acceleration. This naturalistic acceleration profile is from driver experiment data, which lasts around 50 min totally and is shown in **Figure 5**. The maximum and minimum desired acceleration is about 1.1 m/s² and −1.8 m/s², respectively and the vehicle speed varies in the range of 0–33 m/s. This condition can cover a wide range of vehicle dynamics.

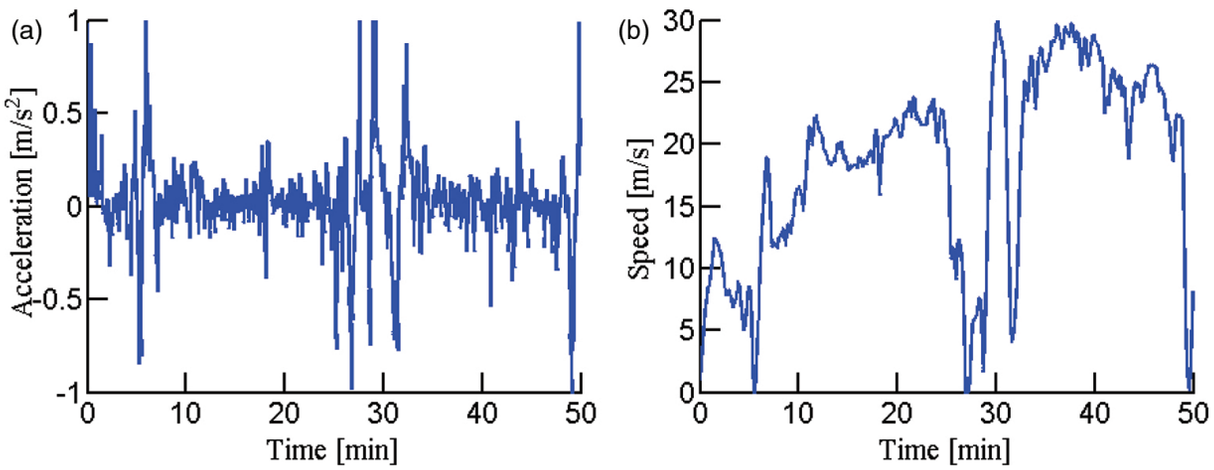

Figure 5. *Reference accele*ration and *speed*. (a) *Accele*ration a*nd* (b) *Veh*icle speed.

Two groups of simulations are conducted: (a) nominal condition; and (b) uncertain condition. Under the nominal condition, all vehicle parameters are shown in **Table 1** and there is no road slope and wind. Under the uncertain condition, the disturbed parameters are vehicle mass, road slope and wind. The maximum value of vehicle mass is used, i.e. M = 1600 kg. The disturbance of road slope is a sinusoidal signal:

$$\varphi = \varphi_{\max} \cdot \sin\left(\frac{2\pi}{T_{\text{slope}}} \cdot t\right) \tag{23}$$

where $\varphi_{\max}$ = 5 deg, and T_{slope} = 50 sec. The disturbance of wind is a periodic triangular signal:

$$v_{\text{wind}} = 2\frac{v_{\text{wmax}}}{T_{\text{wind}}}t - v_{\text{wmax}}, t \in \left[0, T_{\text{wind}}\right), \tag{24}$$

where v_{wmax} = 10 m/s, and T_{wind} = 40 sec.

The simulations results are shown in **Figures 6** and **7**, and to show clearly, only the responses from 0 to 500 sec are plotted as a demonstration. From **Figure 6(a)** and (**b**), under the nominal condition, all three controllers can track the reference acceleration accurately. With the uncertainties, it is found that from **Figure 7(a)** and (**b**) the tracking capability of SMC and H_∞ controller decreases obviously while MMS can still ensure acceptable tracking error. Though switching of controller occurs at both nominal and uncertain conditions (**Figure 6(e)** and **Figure 7(e)**), the control input of MMS behaves continuously and there is no obvious sudden change (**Figure 6(c)** and **Figure 7(c)**). Another concern that must be explained is the spike of acceleration shown in **Figure 6(b)** and **Figure 7(b)**. This is mainly caused by the impact of powertrain when gear switches. A more appropriately designed transmission model could improve the gear-shifting quality.

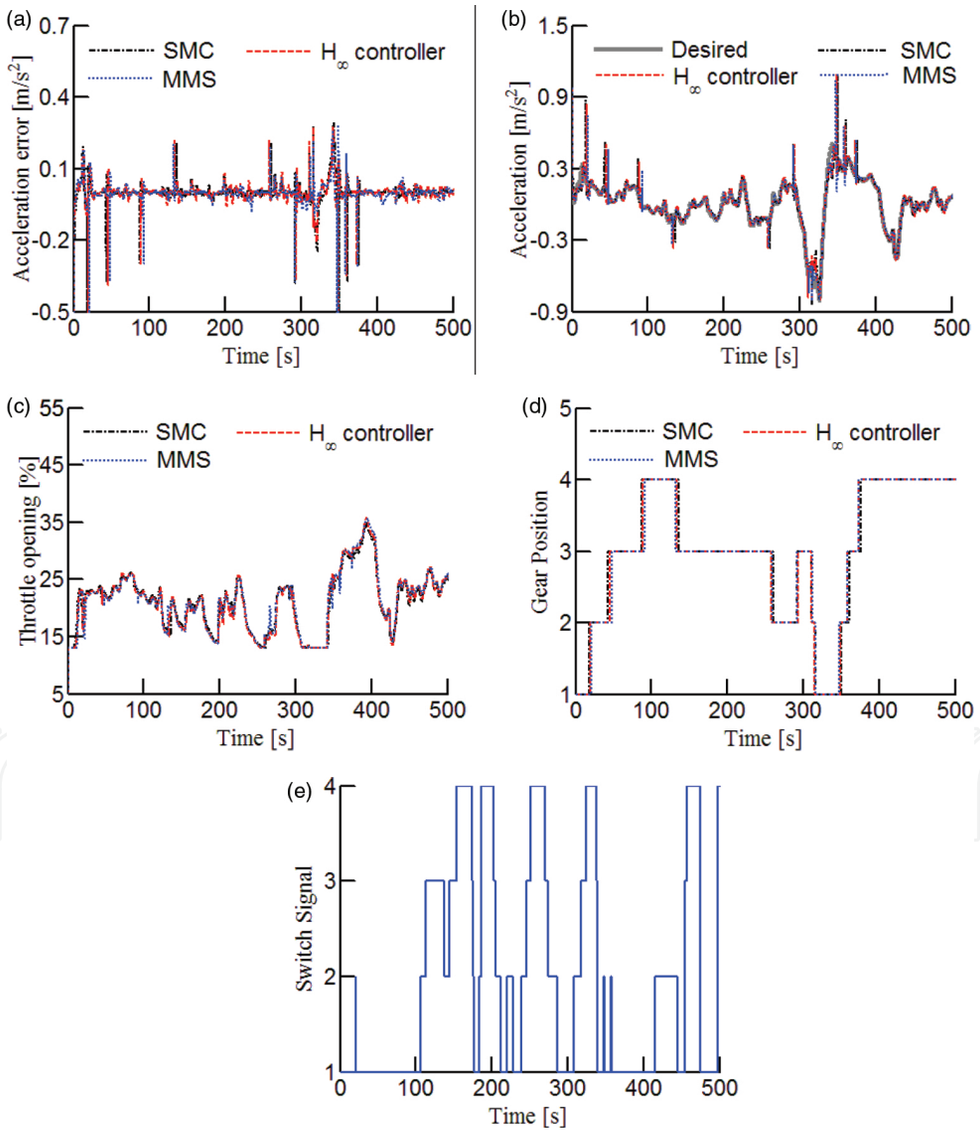

Figure 6. Results under normal condition. (a) Acceleration tracking error, (b) acceleration, (c) throttle control, (d) gear position and (e) switching signal.

http://dx.doi.org/10.5772/63352

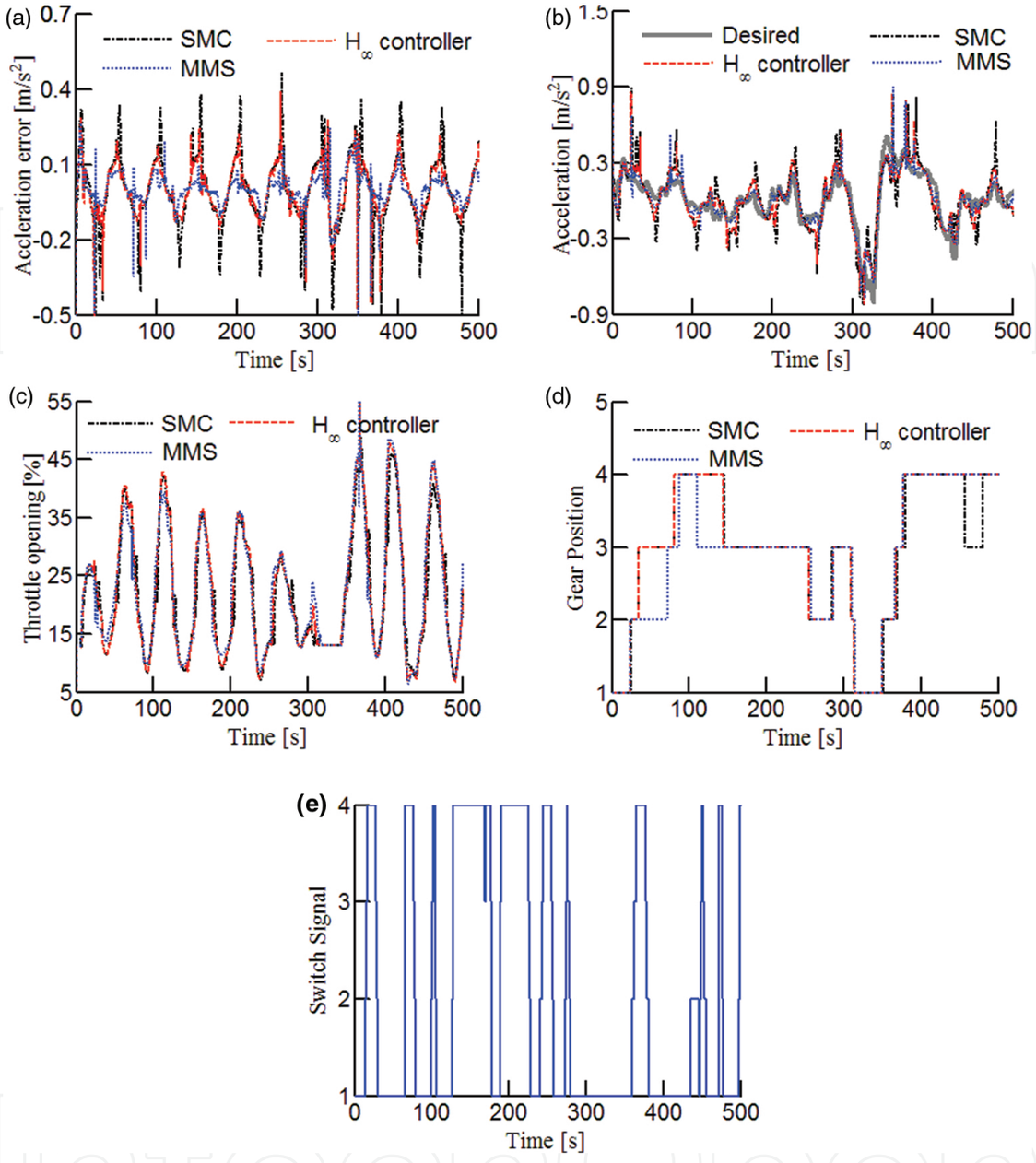

Figure 7. Results under disturbed condition. (a) Acceleration tracking error, (b) acceleration, (c) throttle control, (d) gear position and (e) switching signal.

A more deep simulation is conducted to analyse the influences of uncertain level on the tracking ability of acceleration and gear shifting behaviours. At this condition, the level of uncertainty is increased step by step and the relationship between the uncertain level and model uncertainties is described by:

$$\begin{aligned} M &= 1200\ \text{kg} + 40\text{kg} \cdot \varepsilon,\ \varphi_{\max} \\ &= 1\text{deg} \cdot \varepsilon, v_{\text{wmax}} = 2\frac{\text{m}}{\text{s}} \cdot \varepsilon, \end{aligned} \tag{25}$$

where ε represents the level of uncertainty, with maximum mass 1600 kg, maximum road slope 10 deg, and maximum wind speed 20 m/s (when $\varepsilon = 10$). $\varepsilon = 0$ implies that there is no model uncertainty. The root mean square error (RMSE) of acceleration is used to measure the capability of tracking. **Figure 8** presents the RMSE of acceleration error and the number of gear shifting per minute (denoted as N_{gear}/min). In nominal condition, the RMSE of acceleration error of the three robust controllers is almost the same. As the uncertainty level increases, the tracking capability of the SMC and H_∞ quickly drops, whereas the MMS still holds acceptable accuracy. **Figure 8(b)** is used to release the concern that the MMS might largely increase the number of gear shifting because of its switching structure.

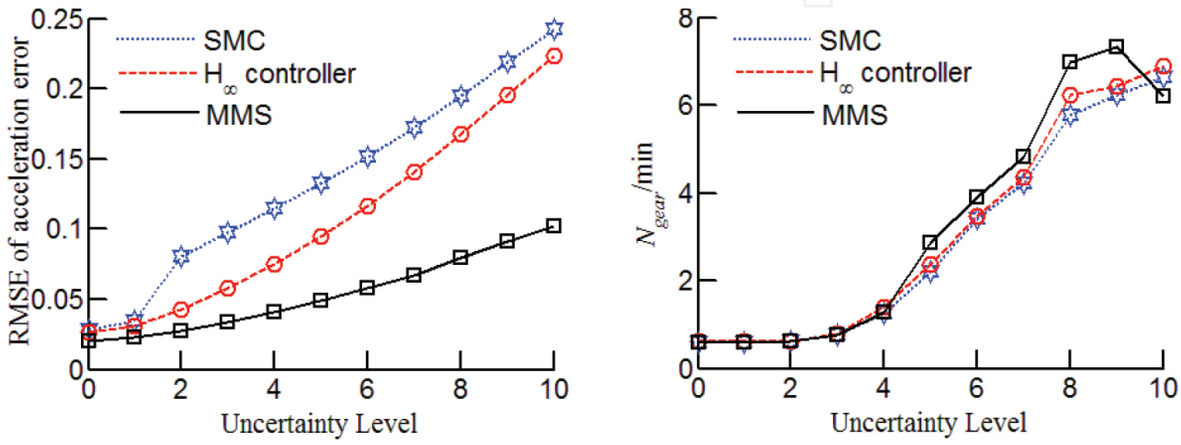

Figure 8. Performances under different uncertain levels.

5. Conclusions

This chapter proposes a robust acceleration control method for consistent node dynamics in a platoon of automated connected vehicles (CAVs). The design, which is based on multiple model switching (MMS) control structure, is able to offer more consistent and approximately linear node dynamics for upper level control design even under large uncertainties, including vehicle parametric variation, varying road slop and strong environmental wind. The following remarks are concluded:

(1) Homogeneous and linear node dynamics is important for platoon control. This requires the acceleration tracking performance to be accurate and consistent, and accordingly results in critical challenges because of the linearization error of powertrain dynamics and large model uncertainties in and around vehicles. The proposed MMS control structure can divide the large uncertainties of vehicle longitudinal dynamics into small ones. Accordingly, multiple robust controllers are designed from the multiple model set, and a scheduling logic is also presented to automatically select the most appropriate candidate controller into loop according to the errors between current vehicle dynamics and models.

(2) The designed switching index can measure the model error of vehicle longitudinal dynamics properly and the right acceleration controller is selected into the closed loop. The robust stability and performance of this acceleration tracking control system can be ensured. Both the simulation and experiment results demonstrate that this switching control system has better performances than that designed by either H_∞ control or sliding mode control approach in large uncertain conditions.

Acknowledgements

This was supported by the State Key Laboratory of Automotive Safety and Energy under Project No. KF16192 and NSF China with grant 51575293.

Author details

Feng Gao[1*], Shengbo Eben Li[2] and Keqiang Li[2]

*Address all correspondence to: gaofeng1@cqu.edu.cn

1 School of Electrical Engineering, Chongqing University, Chongqing, China

2 Department of Automotive Engineering, Tsinghua University, Beijing, China

References

[1] Luettel T, Himmelsbach M, Wuensche J. Autonomous ground vehicles—concepts and a path to the future. Proceedings of the IEEE 100. 2012; (Special Centennial Issue): 1831–1839. DOI: 10.1109/JPROC.2012.2189803.

[2] Shladover S. Longitudinal control of automotive vehicles in close-formation platoons. Journal of Dynamic Systems Measurement and Control. 1991; 113(2): 231–241. DOI: 10.1115/1.2896370.

[3] Sheikholeslam S, Desoer C. Longitudinal control of a platoon of vehicles with no communication of lead vehicle information: a system level study. IEEE Transactions on Vehicular Technology. 1993; 42(4): 546–554. DOI: 10.1109/25.260756.

[4] Hedrick J, Tomizuka M, Varaiya P. Control issues in automated highway systems. IEEE Transactions on Control System Technology. 1994; 14(6): 21–32. DOI: 10.1109/37.334412.

[5] Wang J, Rajamani R. Should adaptive cruise control systems be designed to maintain a constant time-gap between vehicles. IEEE Transactions on Vehicular Technology. 2004; 53(5): 1480–1490. DOI: 10.1109/TVT.2004.832386.

[6] Wang J, Longoria R. Coordinated and reconfigurable vehicle dynamics control. IEEE Transactions on Control System Technology. 2009; 17(3): 723–732. DOI: 10.1109/TCST.2008.2002264.

[7] Gao F, Dang DF, Li SB. Control of a heterogeneous vehicular platoon with uniform communication delay. In: IEEE International Conference on Information and Automation. 8–10 Aug: Lijiang. 8–10 Aug: IEEE; 2015. p. 2419–2424. DOI: 10.1109/ICInfA.2015.7279692.

[8] Stankovic S, Stanojevic M, Siljak D. Decentralized overlapping control of a platoon of vehicles. IEEE Transactions on Control System Technology. 2000; 8(5): 816–832. DOI: 10.1109/87.865854.

[9] Barooah P, Mehta P, Hespanha J. Mistuning-based control design to improve closed-loop stability margin of vehicular platoons. IEEE Transactions on Automatic Control. 2009; 54(9): 2100–2113. DOI: 10.1109/TAC.2009.2026934.

[10] Hao H, Barooah P. Stability and robustness of large platoons of vehicles with double-integrator models and nearest neighbor interaction. International Journal of Robust and Nonlinear Control. 2013; 23(18): 2097–2122. DOI: 1002/rnc.2872.

[11] Rajamani R, Shladover S. An experimental comparative study of autonomous and cooperative vehicle following control systems. Transportation Research Part C. 2001; 9(1): 15–31. DOI: 10.1016/S0968-090X(00)00021-8.

[12] Li ES, Li KJ, Wang JQ. Economy oriented vehicle adaptive cruise control with coordinating multiple objectives function. Vehicle System Dynamics. 2013; 51(1): 1–17. DOI: 10.1080/00423114.2012.708421.

[13] Gao F, Li XP, Ming GQ. Adaptive speed control under vehicle and road uncertainties using multiple model approach. In: American Control Conference; 4–6 June; Portland, OR. 4–6 June 2014: IEEE; 2014. p. 897–902. DOI: 10.1109/ACC.2014.6858598.

[14] Chen Z, Mi C, Xu J, Gong X, You C. Online energy management for a power-split plug-in hybrid electric vehicle based on dynamic programming and neural network. IEEE Transactions on Vehicular Technology. 2014; 63(4): 1567–1580. DOI: 10.1109/TVT.2013.2287102.

[15] Fritz A, Schiehlen W. Automatic cruise control of a mechatronically steered vehicle convoy. Vehicle System Dynamics. 1999; 32: 331–344. DOI: 10.1076/vesd.32.4.331.2077.

[16] Fritz A, Schiehlen W. Nonlinear ACC in simulation and measurement. Vehicle System Dynamics. 2001; 36(2): 159–177. DOI: 10.1076/vesd.36.2.159.3556.

[17] Hunt K, Johansen T, Kalkkuhl J. Speed control design for an experimental vehicle using a generalized gain scheduling approach. IEEE Transactions on Control System Technology. 2000; 8(3): 381–295. DOI: 10.1109/87.845870.

[18] Li SB, Gao F, Cao DP, Li KQ. Multiple model switching control of vehicle longitudinal dynamics for platoon level automation. IEEE Transactions on Vehicular Technology. Forthcoming. DOI: 10.1109/TVT.2016.2541219.

[19] Swaroop D, Hedrick J, Choi S. Direct adaptive longitudinal control of vehicle platoons. IEEE Transactions on Vehicular Technology. 2001; 17(1): 150–161. DOI: 10.1109/CDC.1994.410877.

[20] Higashimata A, Adachi K. Design of a headway distance control system for ACC. JSAE Review. 2001; 22(1): 15–22. DOI: 10.1016/S0389-4304(00)00091-6.

[21] Yamamura Y, Seto Y. An ACC design method for achieving both string stability and ride comfort. Journal of System Design and Dynamics. 2008; 2(4): 979–990. DOI: 10.1299/jsdd.2.979.

[22] Gao F, Li KQ. Hierarchical switching control of longitudinal acceleration with large uncertainties. International Journal of Automotive Technology. 2007; 8(3): 351–359. DOI: 10.1109/ICVES.2006.371597.

[23] Xu Z, Ioannou P. Adaptive throttle control for speed tracking. Vehicle System Dynamics. 1994; 23: 293–306. DOI: 10.1080/00423119408969063.

[24] Keneth J, Tor A, Jens K. Speed control design for an experimental vehicle using a generalized scheduling approach. IEEE Transactions on Control System Technology. 2008; 8(3): 381–395. DOI: 10.1109/87.845870.

[25] Naranjo J, Gonzalez C, Carcia R. ACC+stop&go maneuvers with throttle and brake fuzzy control. IEEE Transactions on Intelligent Transportation System. 2006; 7(2): 213–225. DOI: 10.1109/TITS.2006.874723.

[26] Dai X, Li C, Rad A. An approach to tune fuzzy controllers based on reinforcement learning for autonomous vehicle control. IEEE Transactions on Intelligent Transportation System. 2005; 6(3): 285–293. DOI: 10.1109/TITS.2005.853698.

[27] Hespanha J, Liberzon D, Morse A. Hysteresis-based switching algorithms for supervisory control of uncertain systems. Automatica. 2003; 39: 263–272. DOI: 10.1016/S0005-1098(02)00241-8.

[28] Hespanha J, Liberzon D, Morse A. Multiple model adaptive control. Part 2: switching. International Journal of Robust and Nonlinear Control. 2001; 11(5): 479–496. DOI: 10.1002/rnc.594.

[29] Gao F, Li SB, Kum D, Zhang H. Synthesis of multiple model switching controllers using H∞ theory for systems with large uncertainties. Neurocomputing. 2015; 157: 118–124. DOI: 10.1016/j.neucom.2015.01.029.

[30] Bashivan P, Fatehi A. Improved switching for multiple model adaptive controller in noisy environment. Journal of Process Control. 2012; 22: 390–396. DOI: 10.1016/j.jprocont.2011.12.010.

[31] Kianfar R, Augusto B, Ebadighajari A. Design and experimental validation of a cooperative driving system in the grand cooperative driving challenge. IEEE Transactions on Intelligent Transportation System. 2012; 13(3): 994–1007. DOI: 10.1109/TITS.2012.2186513.

IntechOpen